UNIVERSITY OF BUCHAREST

VIRTUTE ET SAPIENTIA

Faculty of Chemistry
Doctoral School in Chemistry

Thesis Summary

MOF-based and derived catalysts for furanic compounds valorization

PhD student: Mihai Bordeiașu

Supervisors: Prof. Dr. Habil. Simona M. Coman
Prof. UAM Dr. Habil. Joanna Gościańska

Introduction

The doctoral thesis entitled *"MOF-based and derived catalysts for furanic compounds valorization"* presents research conducted in research fields of coordination chemistry, material science, catalysis and biomass valorization. The main objectives include the preparation and comprehensive characterization of metal-organic framework (MOFs)-based materials and MOF-derived hierarchical carbon frameworks, as well as their catalytic application in upgrading bio-based furanic compounds, such as 5-hydroxymehtylfurfural (HMF) and furfural (FAL). Within the context of sustainable development, obtained products are of great importance for industry: FDCA is a promising substitute for terephthalic acid in PET production, HMFCA as a plant-derived precursor for bioactive chemicals, and FOL as a key component in the production of lubricants, synthetic fibers, and vitamin C.

The thesis comprises seven chapters: one theoretical chapter and six chapters dedicated to the objectives, original contributions and conclusions. **Chapter 1** provides an in-depth literature review covering introductory elements in biomass valorization and biorefinery concepts, MOF as a class of materials with emphasis on their catalytic properties, their use as efficient catalysts in furanic compounds valorization, preparation methods for MOF-derived carbon materials and emerging strategies for controlled MOF carbonization. **Chapter 2** outlines the main objectives of the thesis. **Chapter 3** focuses on developing Co-based MOF with different particle morphologies as efficient catalysts in HMF oxidation to HMFCA. **Chapter 4** expands the research by employing Fe-modified ZIF-67 frameworks with different Fe/Co molar ratios as precursors for the preparation of bimetallic Fe/Co carbon materials with hierarchical porosity, synthesized via a SiO_2-assisted method. **Chapter 5** investigates the hydrogenation properties of bimetallic $M_{0.1}Co_{0.9}$-NCF catalysts doped with different secondary metals (Fe, Ni, Cu, and Zn) using molecular hydrogen and alcohols solvents for the efficient hydrogenation of FAL to FOL. **Chapter 6** details experimental procedures, and **Chapter 7** summarizes the results obtained in this PhD thesis, providing a general overview.

1. Bio-based furanic compounds and catalytic valorization on MOF-based materials

Modern society relies heavily on fossil fuels for the production of goods and to satisfy high energy demand [1]. However, as these resources continue to diminish each year, renewable carbon sources are needed to achieve and maintain sustainable development in the industrial sector. In this regard, biomass is a suitable renewable alternative to fossil fuels because it can be found almost anywhere in relatively high amounts, and it can be selected to not compete with food sources [2]. Based on their importance to biorefineries, biomass sources are classified into four main sectors: agriculture, forestry, industry, and aquaculture, and are sorted into dedicated feedstocks (e.g., crops, wood, switchgrass, algae) and residues (crop residues, used oils, wild fruits, urban waste) [3]. Among these, lignocellulosic biomass has gained primary interest because it is a major structural component of plants and is the most abundant terrestrial source. Lignocellulose comprises three biopolymers (lignin, cellulose and hemicellulose) in various proportions depending on the plant type, season, region and climate factors [4]. While lignin has been less studied because of its structural complexity, cellulose fractions are intensively depolymerized and transformed into various chemical compounds, denoted as "platform molecules" owing to their large number of valorization pathways. Two important platform molecules are 5-hydroxymehtylfurfural (HMF) and furfural (FAL). Both furanic compounds are obtained from cellulosic fractions, but in a non-competitive manner: HMF is mostly produced from the dehydration of hexoses [5], while FAL is produced from pentoses found in the hemicellulosic fraction [6]. Their valorization pathways address various industrial sectors, using catalytic reduction, oxidation, amination, or condensation reactions to produce furanic monomers [7, 8], pharmaceutical compounds [9, 10], fungicides [11], or to obtain fuel additives, solvents [12], bio-based diesel and jet fuels [13] (Scheme 1).

Over the last few decades, most of the scientific research on biomass-derived furanic compound valorization has emphasized the use of catalytic systems based on noble metals (Pt, Pd, Ru, Au, Ag) owing to their high activity, as well as some non-noble metals (Fe, Cu, Ni, Co, Sn, Mg, Nb, etc.), for a more economically feasible process [14-18].

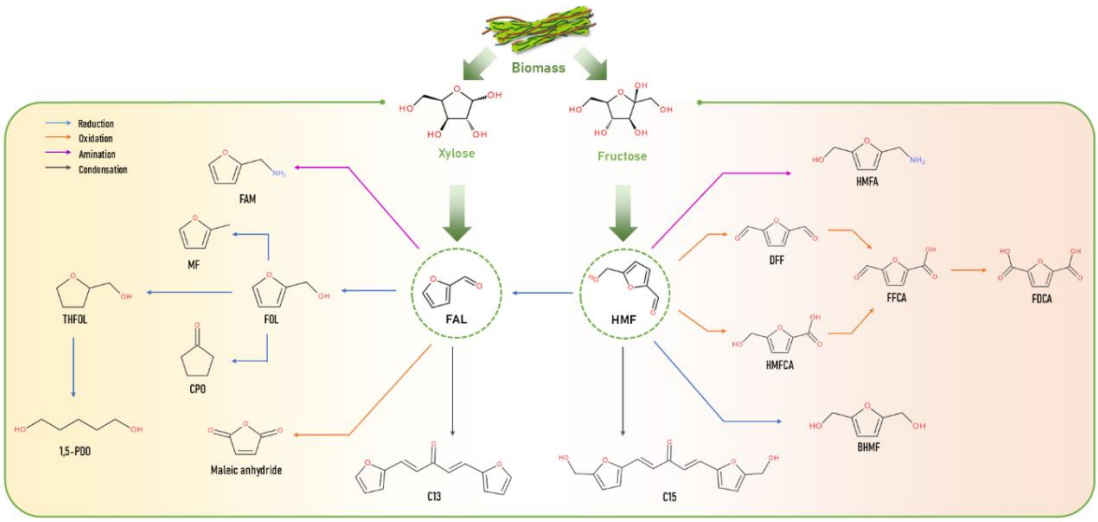

Scheme 1. HMF and FAL valorization pathways to value added-products

In addition to classic catalytic systems, metal-organic frameworks (MOFs) have been considered good candidates for biomass valorization. Within the framework of bio-based furanics valorization, the literature reports highly active MOF systems for the HMF production [21], hydrogenation reactions [22, 23], acetalization of the aldehyde functionality [24], and condensation reactions [25, 26], using either pristine MOFs [21, 24], doped samples [22], composites [26] or MOF-supported noble metal catalysts [23, 27, 28]. However, despite their high activity, MOF are sensitive to temperature, pH variations, and solvents which affect their stability [29]. To overcome these limitations, more stable derived porous carbons (MOF-CMs) have been developed over the last decade using MOFs as sacrificial templates (Figure 1) in a pyrolysis process in air or an inert atmosphere. These materials exhibit higher chemical and hydrothermal stabilities than their precursors while partially retaining their structural properties. Compared with other carbon materials such as carbon nanotubes (CNTs), activated carbon, and graphene, MOF-CMs show higher tunability, similar to their precursors: (1) shapes and pore sizes, which are easily controlled by MOFs; (2) heteroatom doping (mainly N-, P-, and S-) based on linker selection; (3) controllable metal/metal-oxide NP sizes, as a function of pyrolysis conditions; and (4) an overall higher density of active sites with homogeneous distribution due to the preorganized structures of MOF templates [30, 31]. There are several ways to synthesize MOF-CMs, which can be grouped into two main approaches: (i) direct pyrolysis of MOF

precursors and (ii) pyrolysis of MOFs with different additives or composites (guest molecules loaded into MOFs or supported frameworks).

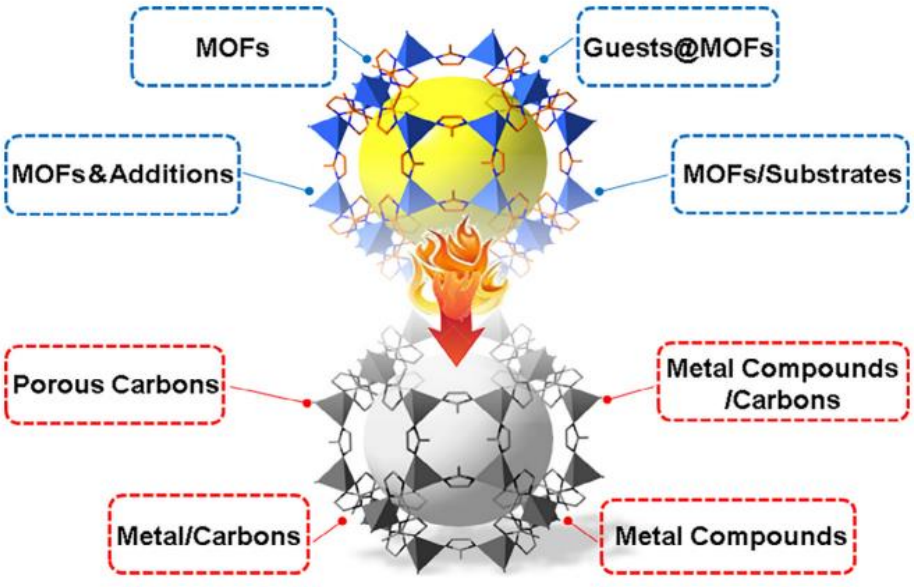

Figure 1. MOF-CMs obtained *via* pyrolysis [32]

Studies have shown that MOF-CMs are promising candidates for applications such as gas storage [33], energy storage [34], electrocatalysis [35] and biomass valorization, particularly upgrading bio-based furanic compounds. Several MOF-CMs containing Fe [36], Co [37, 38], Mn [39], Cu [40] and Ni [41] active phases have been reported in both oxidation and hydrogenation reactions of HMF and FAL, affording promising results while maintaining good stability. However, a major limitation of MOF-CMs is the frequent aggregation of metallic NPs and the predominant microporous structure that occurs during pyrolysis for most of these materials [42]. Consequently, new emerging strategies focused on silica (SiO_2), polymers, or surfactants protective shells [43] have been developed to minimize the technical drawbacks of MOF-CMs, yielding a second generation of carbon materials, MOF-derived carbon nanoframeworks (MOF-CNFs). These materials exhibit better metal dispersion and a hierarchical porous system. Because of their novelty, only a few examples of biomass valorization have been reported [44, 45].

2. PhD thesis objectives

To address the current state-of-the-art and continue the development of MOF-based and derived carbon catalysts for furanic compounds upgrading, the PhD thesis aims to achieve the following objectives: (i) the development of efficient Co-based MOF catalysts for the selective oxidation of bio-based furanic compounds, (ii) the development of efficient bimetallic carbon nanoframeworks for the valorization of bio-based furanic compounds, and (iii) to study the catalytic behavior of bimetallic carbon nanoframeworks in the valorization of bio-based furanic compounds and establish correlations between their structural properties and catalytic efficiency.

To achieve these objectives, three main strategies were employed (Figure 2; the circled numbers correspond to the chapters in the thesis where the respective transformation is studied). First, Co-based MOF materials with different morphologies were prepared using various cobalt sources, organic ligands, and modulators. The obtained materials were used as catalysts for the selective oxidation of HMF to HMFCA, followed by oxidation to FDCA (Figure 2, step 3).

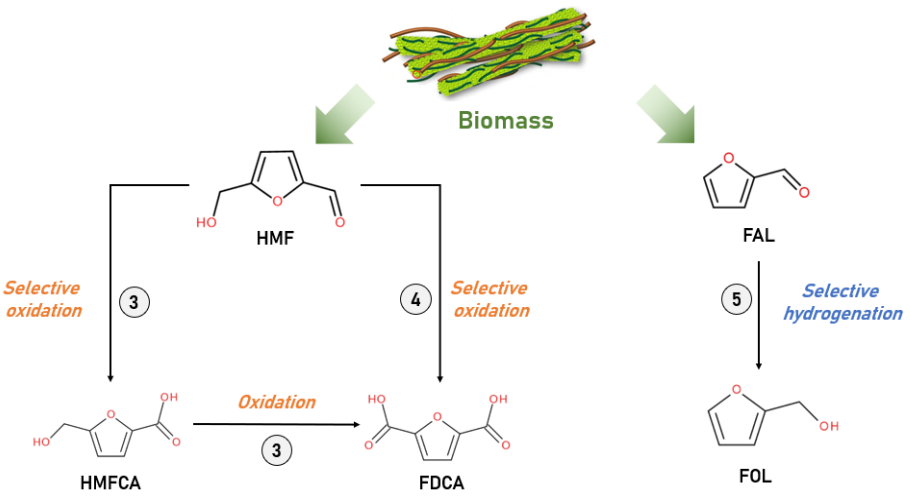

Figure 2. Proposed strategies for the catalytic upgrading of biomass-derived furanic compounds

Further studies have focused on the preparation of bimetallic carbon nanoframeworks containing cobalt and small amounts of secondary metal dopants. These carbon materials were prepared using both conventional and silica-assisted methods and tested in the selective oxidation reaction of HMF to FDCA (Figure 2, step 4) and the hydrogenation of FAL to FOL (Figure 2, step 5).

3. Co-based MOFs for HMF catalytic oxidation

This chapter encompasses the results of the preparation, characterization, and catalytic testing of Co-based MOFs with different particle morphologies. For this purpose, four different Co-based MOF samples were prepared under solvothermal conditions using the classic self-assembly of Co^{2+} with nitrogen-containing linkers (2-methylimidazole, 2mim) and oxygen-containing linkers (1,3,5-benzentricarboxylic acid, H_3BTC), with the addition of modulators or by employing a ligand exchange approach. Moreover, a core-shell structure was obtained using Co_3O_4 as the cobalt source and H_3BTC linker. To assess their structural features, the prepared samples were characterized using several techniques, such as XRD, DRIFT, SEM, N_2 adsorption-desorption isotherms, TGA, and NH_3-/CO_2-TPD.

ZIF-67 exhibits a dodecahedral particle shape (Figure 3A), which is well known in the literature [46] and is characterized by a large specific surface area (1169 m^2/g), but is mostly microporous. By comparison, the Co_3O_4@Co-BTC sample has the lowest specific surface area (24 m^2/g), but a large volume of mesopores and a unique anemone-like particle morphology (Figure 3D), which enfolds a high density of surface active sites, providing a different perspective for the catalytic behavior.

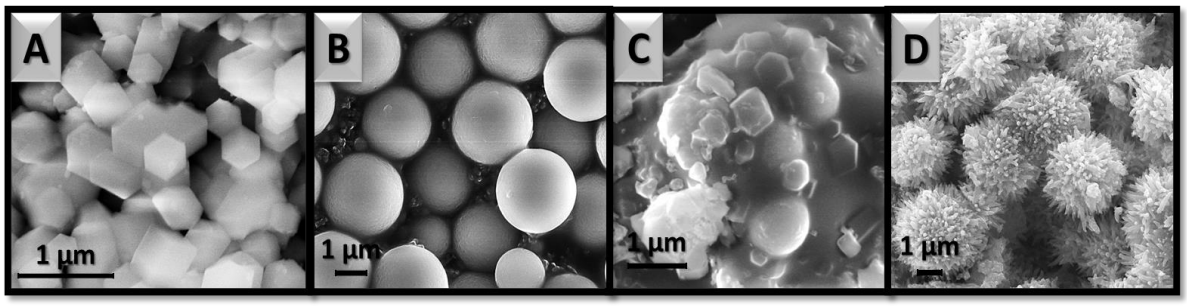

Figure 3. SEM images of ZIF-67 (A), Co-BTC (B), Co-BTC-2mim (C) and Co_3O_4@Co-BTC (D)

HMF oxidation can proceed though different initial pathways occurring at aldehyde or alcohol functionalities, giving rise to furanic compounds or can undergo C-C bond cleavage yielding to small carboxylic acids (Figure 4A) [47]. Thus, selective oxidation requires highly selective catalysts that can convert HMF before its degradation [48], while maintaining good stability.

Initial catalytic tests revealed that in the presence of H_2O_2 as an oxygen donor and water as a solvent, a significant fraction of the Co-based MOFs structure was destroyed, most probably due to the gradual replacement of the metal-coordinated linkers by water molecules [49]. However, using *tert*-butyl hydroperoxide (TBHP) as the oxidant and acetonitrile (ACN) as the solvent provides a suitable medium for high selectivity to the targeted products and stability of the catalyst.

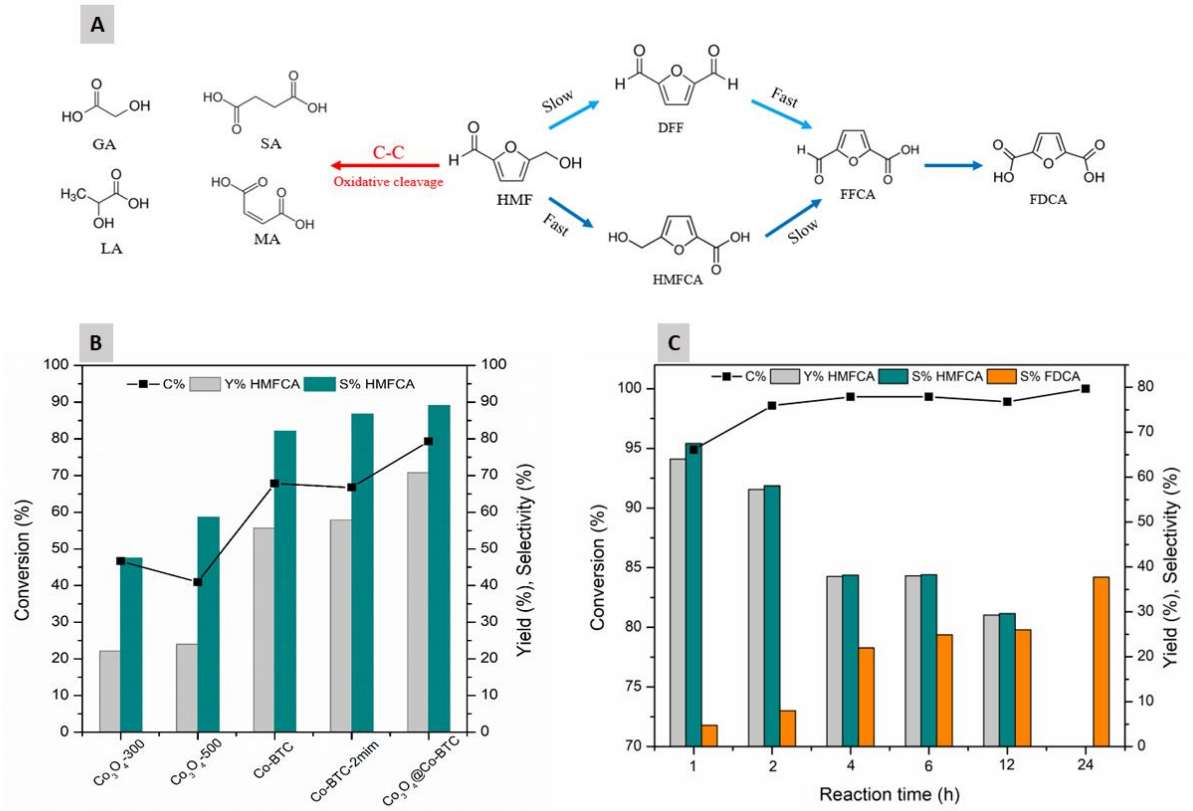

Figure 4. Reaction pathways for selective oxidation and oxidative cleavage of HMF (A), HMF conversion and selectivity/yield to HMFCA in the presence of Co-based MOFs and Co_3O_4 oxides (B) and time evolution of HMF oxidation to HMFCA and FDCA on Co_3O_4@Co-BTC (C). *Reaction conditions: 0.2 mmol HMF, 1.87 mmol TBHP, 5 mg catalyst, 4.4 mL ACN, 60°C, 1h (B), 0.2 mmol HMF, 1.87 mmol, 25 mg Co_3O_4@Co-BTC, 4.4 mL ACN, 100°C (C).*

Under very mild reaction conditions, high catalytic efficiency for the Co-based MOFs was observed (Figure 4B), with conversion values in the 47.7-79.3% range and selectivity of 82.1-89.1%. Among all the tested materials, Co_3O_4@Co-BTC, characterized by a unique particle morphology, was found to be the most efficient catalyst. Further adjustments of the reaction conditions (Figure 4C) revealed the great flexibility of this sample to further oxidize HMFCA to

FDCA over a period of 24h, affording a complete HMF conversion and a selectivity to FDCA of 37.7%, alongside large amounts of degradation products (Figure 4A).

4. Fe,Co-MOF-derived carbon nanoframeworks for HMF catalytic oxidation

This chapter presents further results dedicated to the preparation and exhaustive characterization of ZIF-derived bimetallic N-doped porous carbons (NPCs) and N-doped carbon nanoframeworks (NCFs) (Scheme 2). Following annealing at high temperatures in an inert atmosphere, bimetallic Fe_xCo_y-ZIF with different loadings resulted in highly dispersed Fe and Co nanoparticles embedded in an N-doped carbon matrix (Fe_xCo_y-NPCs). Employing the emerging SiO_2-assisted methodology, a series of Fe_xCo_y-NCF catalysts was obtained.

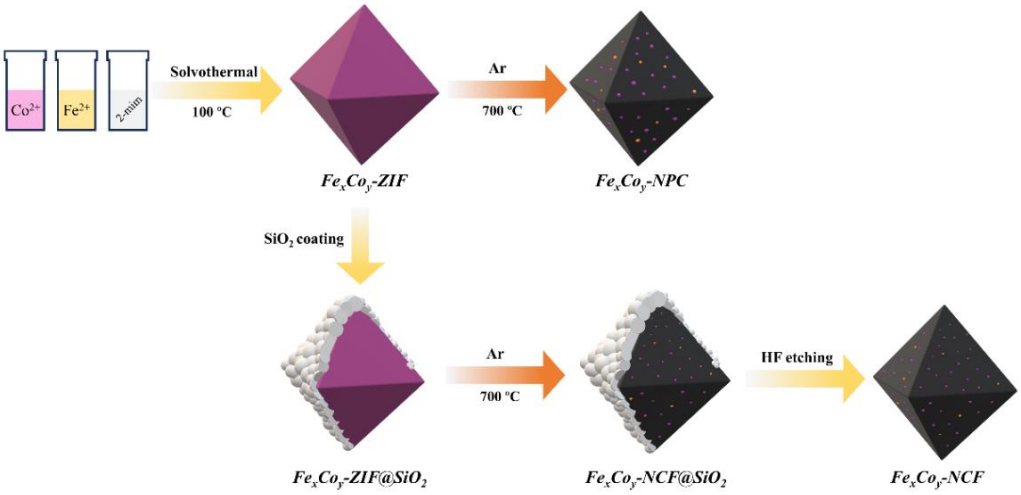

Scheme 2. Synthetic procedure of bimetallic Fe_xCo_y-NPC and Fe_xCo_y-NCF catalysts

Various characterization techniques, such as XRD, FTIR, and Raman spectroscopy, revealed better structuring of the carbon matrix and finer metal dispersion with smaller crystallite sizes [50] for the NCFs, highlighting the importance of SiO_2 in generating carbon nanoframeworks. Additional textural properties of the investigated samples revealed a significant drop in the specific surface area during the carbonization of ZIF precursors, from 990-1279 m^2/g to 138-315 m^2/g in the case of Fe_xCo_y-NPC materials and 307-376 m^2/g for Fe_xCo_y-NCF, but with an increased external surface area as a result of mesopores generation. Typically, Fe_xCo_y-NCF exhibited larger mesopore volumes (0.24-0.65 cm^3/g) and pore diameters (4.7-7.2 nm),

which are essential for the valorization of biomass-derived compounds, such as HMF. Moreover, the presence of the SiO_2 shell during carbonization minimized nitrogen loss, facilitating higher concentrations of base sites in the Fe_xCo_y-NCF samples, accounted for 0.488-0.563 mmol CO_2/g.

The catalytic tests revealed high activity for both NPC and NCF catalysts, affording more than 86.7% HMF conversion (Table 1), but with significant differences in selectivity. The unmodified samples produced only HMFCA with selectivities of 61.3% for Co-NPC (Table 1, entry 6) and 86.7% for Co-NCF (Table 1, entry 2), respectively. The presence of iron species on the surface of the catalyst was found to be a key element for the overoxidation to FDCA, affording selectivities in the 50-82.4% range (Table 1, entries 3-5).

Table 1. Fe_xCo_y-NCF catalytic efficiency in HMF oxidation to FDCA

Entry	Catalyst	X_{HMF}, %	S_{HMFCA}, %	S_{FDCA}, %	XPS Co (at.%)	XPS Co^{2+}/Co^0 ratio	XPS Fe (at.%)	XPS Fe^{2+}/Fe^{3+} ratio
1	None	< 1	< 0.5	0	-	-	-	-
2	Co-NCF	86.7	86.7	0	2.75	2.02	-	-
3	$Fe_{0.05}Co_{0.95}$-NCF	99.8	2.4	50.0	3.38	2.01	1.30	0.70
4	$Fe_{0.10}Co_{0.90}$-NCF	> 99.9	0	80.5	2.84	2.20	2.57	0.42
5	$Fe_{0.15}Co_{0.85}$-NCF	> 99.9	0	82.4	6.38	3.28	3.30	0.50
6	Co-NPC	88.4	61.3	0	n.d.	n.d.	-	-
7	$Fe_{0.10}Co_{0.90}$-NPC	95.4	10.2	32.9	10.89	0.08	0.70	0.37

Reaction conditions: 1mmol HMF, 7.26 mmoles TBHP, 25 mg catalyst, 5 mL ACN, 80°C, 6h. Note: the difference till 100% represents the selectivity to degradation products. n.d. – not determined

Although highly active, the recycling experiments showed a rapid loss of activity at the iron sites. The low stability of the Fe-N_x sites could be explained by several degradation routes, such as oxidative attack by peroxides [51], carbon matrix corrosion [52], and dissolution of iron from the Fe-N_x sites [53]. Quantitative and qualitative Fe and Co determinations showed no metal leaching. However, post-reaction DRIFT and XPS analyses revealed the presence of coordinated OH species, which altered the local electronic properties of the active sites, expressed as modifications in the Fe^{2+}/Fe^{3+} and pyridinic-N/pyrrolic-N ratios. These results support a combined deactivation mechanism that includes both iron oxidation and N-pyrrolic degradation via N-protonation during the decomposition of the TBHP oxidant.

The efficiency of the catalyst could only be partially restored through subsequent reduction with $NaBH_4$.

5. Bimetallic ZIF-derived carbon nanoframeworks for FAL hydrogenation

This chapter expands the catalytic applicability of $M_{0.1}Co_{0.9}$-NPC and $M_{0.1}Co_{0.9}$-NCF materials in the selective FAL hydrogenation to FOL using various dopants (M = Fe, Ni, Cu, Zn). The incorporation of various metals into ZIFs results in variations in the framework flexibility and aperture size [54], namely, a minor framework expansion (Figure 5A, d_{002} line, inset). The minor flexibility induced significant modifications in the derived carbon materials, affecting the dispersion of active sites and Co particle sizes (Figure 5B) [55]. Further adsorption-desorption experiments revealed better textural and acid-base properties for the NCF series, characterized by larger mesopore volumes and pore diameters with dopant-dependent variations. The higher nitrogen content of the NCF samples induced a higher concentration of surface base sites and provided strong anchoring points for metal nanoparticles, influencing both stability and a highly uniform distribution on the carbon matrix [56].

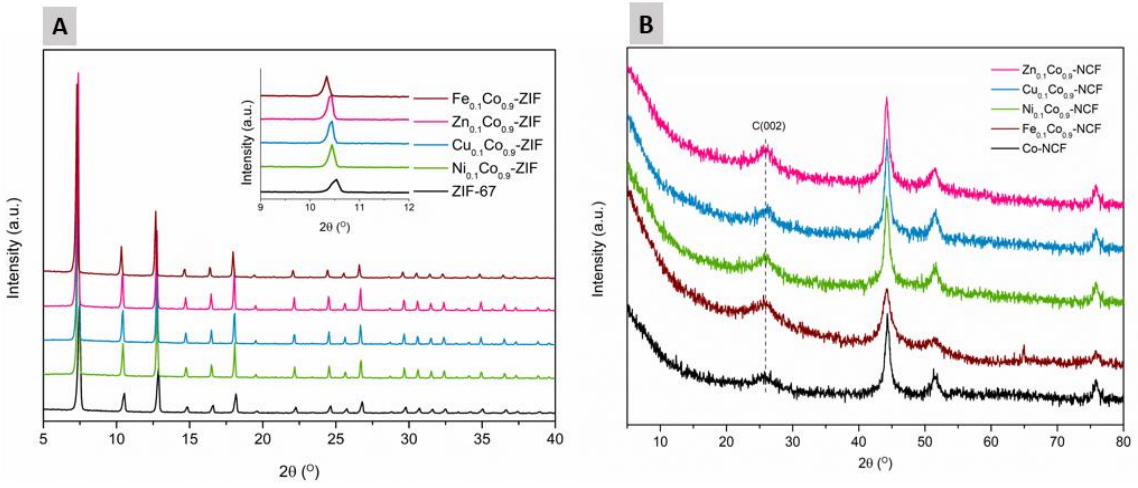

Figure 5. XRD patterns of bimetallic $M_{0.1}Co_{0.9}$-ZIFs (A) and $M_{0.1}Co_{0.9}$-NCFs (B)

FAL hydrogenation can be carried out at the aldehyde and/or furan groups, alongside hydrodeoxygenation or ring opening, as a function of hydrogen pressure, solvent, temperature, and catalyst nature [57]. Therefore, the initial catalytic tests focused on optimizing reaction.

Temperature and hydrogen pressure significantly affect the product selectivity and FAL conversion. At 100°C and 15 bar H_2, using ethanol as a solvent, the formation of side products can be greatly inhibited while ensuring good conversion. On the other hand, the solvent is critical for the hydrogenation of FAL to FOL. Contrary to general expectations, alcohols outperformed aprotic and nonpolar solvents, contributing to >97% selectivity to FOL.

Under the optimized reaction conditions, all the prepared catalysts were screened (Table 2). The catalytic results showed that the presence of the dopant significantly affected the catalytic efficiency of $M_{0.1}Co_{0.9}$-NCF. For the $Ni_{0.1}Co_{0.9}$-NCF and $Fe_{0.1}Co_{0.9}$-NCF samples, a significant improvement in the FAL conversion and FOL selectivity was observed (Table 2, entries 2 and 3), whereas both the $Cu_{0.1}Co_{0.9}$-NCF and $Zn_{0.1}Co_{0.9}$-NCF samples afforded lower conversions (Table 2, entries 4 and 5), and the selectivity for FOL decreased significantly in favor of acetals and diols.

Table 2. Catalyst screening in FAL hydrogenation to FOL

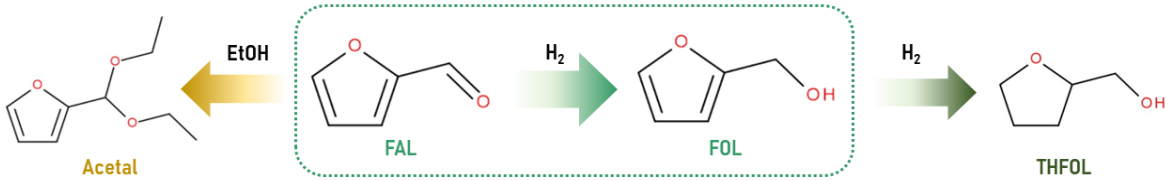

Entry	Catalyst	X_{FAL} (%)	S (%)			
			FOL	THFOL	Acetal	Others
1	Co-NCF	84.4	99.5	0.5	0	0
2	$Fe_{0.1}Co_{0.9}$-NCF	99.9	99.4	0.6	0	0
3	$Ni_{0.1}Co_{0.9}$-NCF	95.0	97.0	1.3	1.1	0.6
4	$Cu_{0.1}Co_{0.9}$-NCF	78.8	88.9	0	0	11.1
5	$Zn_{0.1}Co_{0.9}$-NCF	69.0	64.3	0	18.7	17.0
6	Co-NPC	99.5	96.4	1.9	0	1.7
7	$Fe_{0.1}Co_{0.9}$-NPC	51.7	86.9	0.3	12.8	0
8	$Ni_{0.1}Co_{0.9}$-NPC	99.7	96.6	1.8	0	1.6
9	$Cu_{0.1}Co_{0.9}$-NPC	98.5	97.0	1.6	0	1.4
10	$Zn_{0.1}Co_{0.9}$-NPC	89.3	97.4	1.0	1.6	0

Reaction conditions: 1 mmol FAL, 20 mg catalyst, 15 bar H_2, 3h, 100°C, 4 ml EtOH. Others: 1,5-pentanediol, 1,4-pentanediol, 1,2-pentanediol, hemiacetals

For the $M_{0.1}Co_{0.9}$-NPC samples, a high conversion of FAL and relatively constant selectivity to FOL were recorded (Table 2, entries 6-10). These results can be mainly attributed to the larger amounts of Co found in the samples, whereas the impact of the dopant cannot be properly attributed. Only in the case of $Fe_{0.1}Co_{0.9}$-NPC, the lower conversion (51.7%) and selectivity to FOL (86.9%) can be attributed the larger Fe particles.

6. Experimental section: reagents, methodologies, instrumentation

This chapter presents in detail all the applied synthesis methodologies, characterization techniques, catalytic testing conditions, and products analysis and quantification.

Co-based MOF catalysts were prepared under solvothermal conditions using $Co(NO_3)•6H_2O$ or Co_3O_4 as metal precursors and 2-methylimidazole (2mim) and 1,3,5-benzentricarboxylic acid (H_3BTC) as organic linkers. The synthesis was carried out in a Teflon-lined stainless-steel autoclave using different temperatures and modulators to induce various particle morphologies.

Bimetallic ZIF templates were obtained in similar conditions, using various ratios of dopants and cobalt. Bimetallic nitrogen-doped carbon materials (NPCs) and nitrogen-doped carbon nanoframeworks (NCFs) were obtained by thermally annealing ZIF templates under a constant argon flow. For the NCF series, additional SiO_2 coating and post-carbonization SiO_2 etching steps are described.

The complete catalysts characterization was assessed using various techniques, namely XRD, DRIFT, FTIR, Raman, N_2 adsorption-desorption measurements, CO_2- and NH_3-TPD, TG-DTA, elemental analysis, XPS, SEM-EDX, and ICP-OES.

Catalytic tests were typically carried out in stainless-steel autoclaves using different amounts of substrates (HMF and FAL), catalysts, solvents, oxidants (TBHP), hydrogen sources (H_2 pressures), temperatures, and reaction times. Prior to analysis, the recovered products were silylated with 1 wt./wt.% of trimethylchlorosilane in 99% of N,O-Bis(trimethylsilyl)-trifluoroacetamide (BSTFA:TMCS), diluted with ethyl acetated and examined on a gas chromatograph equipped with a flame-ionization detector (GC-FID). Products identification was performed using a gas chromatography - mass spectrometry (GC-MS).

7. General conclusions and future perspectives

Biomass-derived furanic compounds have emerged as pivotal molecules in the transition towards a more sustainable chemical industry. FAL and HMF are two of the most versatile platform molecules available, originating from distinct lignocellulosic fractions (i.e., hexoses and pentoses). Their structures, which are rich in oxygen-containing functionalities, can facilitate the production of a broad spectrum of chemical compounds. However, the targeted selective transformation of FAL and HMF into key compounds requires catalytic pathways to increase productivity and minimize side reactions.

In this context, the studies presented in this doctoral thesis collectively explored how MOFs, as a class of hybrid materials, as well as their derived carbon materials, can be rationally designed to catalyze the selective upgrading of biomass-derived furanic compounds. Altogether, these studies emphasize the structural tunability of MOFs, the robustness of carbonized derivatives, and the synergy between cobalt and other metals as key elements in engineering efficient catalytic systems capable of operating under the demanding solvothermal conditions associated with biomass valorization.

Overall, the present doctoral thesis provides original contributions to the field, demonstrating that Co-MOFs and their derived carbon materials constitute a highly adaptable class of catalysts for the valorization of furanic compounds. Through engineered synthesis, hierarchical structuring, and strategic metal incorporation, these materials can be optimized to achieve high activity, selectivity, and stability in the transformation of furanic platform molecules into value-added products.

Although the studies conducted within the doctoral thesis scope provided in-depth investigations, future research perspectives remain open. The high applicability of Fe_xCo_y-NCF opens up prospects for other reactions of furanic compounds, such as reductive amination, condensation, and selective ring-opening of the furanic core, as well as for other types of biomass-derived platform molecules, such as levulinic and succinic acids or aliphatic polyols. In addition, the stabilization of Fe-N_x species in these catalysts provides another fruitful research direction for future studies. Finally, from a broader technological perspective, the integration of these catalysts into continuous-flow systems represents a compelling opportunity.

The experimental data of the doctoral thesis can be found in the following articles:

1. M. Bordeiasu, A. Ejsmont, J. Goscianska, B. Cojocaru, V. I. Parvulescu, S. M. Coman, Catalytic oxidation of biomass-derived 5-hydroxymethylfurfural to 5-hydroxymethyl-2-furancarboxylic acid by Co-based MOFs, Appl. Catal. A.-Gen, 2023, 657, 119147. (IF = 4.8)

2. M. Bordeiasu, J. Goscianska, R. Panek, A. Nicolaev, B. Jurca, V. I. Parvulescu, S. M. Coman, Magnetic Fe,Co-Nanocarbon Frameworks Derived from Fe-Doped Zeolitic Imidazolate Framework-67 as Highly Active Catalysts for 5-Hydroxymethylfurfural Oxidation, ChemSusChem, 2025, 18, e202500678. (IF = 6.6)

3. M. Bordeiasu, J. Goscianska, A. Nicolaev, S. A. Nicolae, M. C. Istrate, B. Cojocaru, B. Jurca, V. I. Parvulescu, S. M. Coman, Iron as an Efficient Dopant in Co-N-Carbon Frameworks for Highly Selective Furfural Hydrogenation, Appl. Catal. A.-Gen, 2026, 725, 121138. (IF = 4.8)

Selective references

1. S. Fernando *et al.*, Energy Fuels, 2006, 20, 1727-1737
2. D. W. Rackemann & W. O. S. Doherty, Biofuel Bioprod. Biorefin., 2011, 5, 198-214
3. F. Cherubini *et al.*, Biofuel Bioprod. Biorefin., 2009, 3, 534-546
4. H. Jørgensen *et al.*, Biofuel. Bioprod. Biorefin., 2007, 1, 119-134
5. R.-J. van Putten *et al.*, Chem. Rev., 2013, 113, 1499-1597
6. L. T. Mika *et al.*, Chem. Rev., 2018, 118, 505-613
7. H. Hirai, J. Macromol. Sci. A, 1984, 21, 1165-1179
8. Y.-Z. Qin *et al.*, Green Chem., 2015, 17, 3718-3722
9. A. C. Braisted *et al.*, J. Am. Chem. Soc., 2003, 125, 3714-3715
10. N. S. Gould *et al.*, ChemCatChem, 2020, 12, 2106-2115
11. G.D. Yadav & R. V. Sharma, Appl. Catal. B: Environ., 2014, 147, 293-301
12. J.-P. Lange, Catal. Today, 2024, 435, 114726
13. A. Tampieri *et al.*, Appl. Catal. B: Environ., 2021, 282, 119599
14. A. Tirsoaga *et al.*, Appl. Catal. B: Environ., 2020, 278, 119309
15. M. J. Gilkey & B. Xu, ACS Catalysis, 2016, 6, 1420-1436
16. M. Sajid *et al.*, Green Chem., 2018, 20, 5427
17. P. L. Arias *et al.*, Catal. Sci. Technol., 2020, 10, 2721-2757
18. R. Ahorsu *et al.*, Ind. Eng. Chem. Res., 2021, 60, 18612-18626
19. H.-C. Zhou *et al.*, Chem. Rev., 2012, 112, 673-674
20. H. Daglar & S. Keskin, Coord. Chem. Rev., 2020, 422, 213470
21. Y. Zhang *et al.*, AIChE J., 2023, 69, e17890
22. J. Tan *et al.*, Catalysts, 2024, 14, 929
23. Q. Yuan *et al.*, J. Mol. Catal. A Chem., 2015, 406, 58-64
24. A. Franco *et al.*, Appl. Mater. Today, 2024, 39, 102266
25. D. de la Flor *et al.*, J. Catal., 2021, 401, 27-39
26. G. Morales *et al.*, Fuel, 2023, 339, 127465
27. K. Zhang *et al.*, ACS Sustain. Chem. Eng., 2022, 10, 10286-10293
28. X. Li *et al.*, Appl Catal. A-Gen, 2019, 575, 152-158
29. A. Howarth *et al.*, Nat. Rev. Mater., 2016, 1, 15018

30. J. Wang *et al.*, Nanoscale, 2020, 12, 4238-4268
31. H. Konnerth *et al.*, Coord. Chem. Rev., 2020, 416, 213319
32. Y.-Z. Chen *et al.*, Coord. Chem. Rev., 2018, 362, 1-23
33. G. Srinivas *et al.*, Energy Environ. Sci., 2014, 7, 335-342
34. T. Wang *et al.*, J. Am. Chem. Soc., 2018, 140, 6130-6136
35. A. Ejsmont *et al.*, J. Colloid Interface Sci., 2024, 653, 1326-1338
36. R. Fang *et al.*, Green Chem., 2016, 18, 3152-3157
37. Y. Shang *et al.*, Ind. Eng. Chem. Res., 2020, 59, 6532-6542
38. Y. Feng *et al.*, J. Catal., 2020, 381, 570-578
39. P. Wang *et al.*, Eur. J. Inorg. Chem., 2024, 28, e202400642
40. Z.-F. Li *et al.*, Mol. Catal., 2022, 518, 112092
41. H. Xia *et al.*, Inorg. Chem. Commun., 2021, 133, 108894
42. W. Zhong *et al.*, ACS Catal. 2015, 5, 1850-1856
43. C. Wang et al., Chem, 2020, 6, 19-40
44. M. Huai *et al.*, ChemCatChem, 17, 2025, e202401651
45. Y. Wu *et al.*, Sci. China Chem., 2022, 65, 2450-2461
46. H. Pan *et al.*, Cryst. Growth Des., 2020, 20, 6689-6690
47. M. El Fergani *et al.*, Catal. Today, 2022, 405- 406, 267-276
48. T. Pasini *et al.*, Green. Chem., 2011, 13, 2091-2099
49. S. Yuan *et al.*, Adv. Mater., 2018, 30, 1704303
50. H. Wang *et al.*, ACS Appl. Mater. Interfaces, 2020, 12, 34021
51. C. H. Choi *et al.*, Energy Environ. Sci., 2018, 11, 3176-3182
52. C. H. Choi *et al.*, Angew. Chem. Int. Ed., 2015, 54, 12753-12757
53. C. H. Choi *et al.*, ACS Catal., 2016, 6, 3136-3146
54. P. Krokidas *et al.*, Phys. Chem. Chem. Phys., 2018, 20, 4879-4892
55. L. Shang *et al.*, Adv. Mater., 2016, 28, 1668-1674
56. Q. Lu *et al.*, ACS Catal., 2022, 12, 1364-1374
57. J.-J. Tan *et al.*, J. Fuel. Chem. Technol., 2021, 49, 780-790